

DESIGN AND ANALYSIS OF A FLYBACK CONVERTER WITH IMPROVED SNUBBER CELLS

^{#1}SRAVAN KUMAR PURELLA, *Research Scholar,*

^{#2}Dr. ARRAMARAJU PRASAD RAJU, *Supervisor,*

^{#3}Dr. K. PRAKASH, *Co-Supervisor,*

Department of Electrical and Electronics Engineering,

NIILM UNIVERSITY, KAITHAL, HARYANA, INDIA.

ABSTRACT: Flyback converters are widely used in modern industrial systems, particularly in low-power applications, because of their simple design and management. Furthermore, the following characteristics have been prioritized: the ability to adapt to changing power requirements, the ability to function at various output levels using a single unit, ease of installation, cost adherence, isolation between the circuit structure's inputs and outputs, and compliance with standard safety regulations. Despite its benefits, the application of flybacks is difficult due to the presence of leaky inductors. They produce severe voltage spikes and additional power loss. Our flyback-based circuit technique enhances performance by minimizing losses and offering many voltage levels from a single power source. Furthermore, it improves performance by lowering voltage strain on semiconductors. These innovations provided all of the required analog and numerical measurements. These conclusions were based on standard circuit modeling. Next, the focus shifts to lowering losses and increasing circuit efficiency. By dividing 5 volts by 1 amp and 12 volts by 1 amp, two distinct and independent output voltage sources are created.

Keywords: Flyback converter, power supply, snubber circuits.

1.INTRODUCTION

DC-DC adapters are getting increasingly popular. Energy efficiency is critical for both technological growth and social wellbeing. The growing demand for energy has pushed it to the level of global concern. Isolation is also an important aspect of electrical safety. Phase-width modulated (PWM) DC-DC converters are simple to use, quick to respond, and simple to build in the industrial sector. Differentiating "isolated" and "non-isolated" DC-DC converters. Buck, boost, and buck-boost converters are widely used in many industries because to their simple design and high efficiency. Concerns about the isolation of these groups are genuine. Forward and reverse converters provide circuit isolation. Forward and flyback converters work similarly, while buck-boost and flyback converters work differently.

When developing isolated converters, it is critical to choose the appropriate core and transformer

construction. Flyback converters are more efficient than forward converters because the primary and secondary windings operate simultaneously. Current in the primary winding is equal to current in the magnetizing winding. Forward-facing inverters contain three windings. Flyback converters are used in industrial equipment because of their simple management. However, poor inductance causes higher power loss in flyback converters. Flyback converters are used to ensure seamless transitions. Inadequate snubber cell selection for flyback converters causes increased voltage strains and losses. As a result, external cooling systems are required, along with the associated costs. Because of their inefficiency, flyback converters are limited to low-power applications. Passive snubber circuits should be used on both input and output. However, because of the increasing number of components and frequency intervals, these converters generate less EMI and experience more losses.

DCM and CCM use the magnetizing inductance to reset the current during the transition phase. The CCM's continual operation causes energy to be transferred during the transition. As a result, they are used in circumstances that require substantial power. At this point in the operation, no energy is transferred from the input to the output, and the current is negative. To reduce reverse recovery losses, diodes are toggled successively. DCM is thus superior to CCM. The converter's efficiency can be improved by selecting the appropriate snubber cells. Configuring a split-flyback conversion snubber. The principal snubber cell is connected to the main windings via a fast diode, reducing switch voltage stress. Phasing devices that use parallel diodes are known as light snubber cells. The efficiency of the flyback converter is determined by the value of the snubber cell.

This study studies and builds a flyback converter with the necessary snubber cells to properly address the aforementioned issues. This effort validates the theoretical analysis by building a real-world circuit. Different circuit outputs have distinct voltage and current characteristics. The 5V/1A output stands in contrast to the 12V/1A output. The circuit is supplied with 310 volts direct current. This voltage is obtained by dividing 138 by 66 kHz. Passive snubbers that change the switching frequency twice might generate external stress and cause delays. Consequently, movable external switching cells may be required. In this experiment, the snubber circuit works well even when there are no soft switching cells at different frequencies. We can disassemble the snubber circuits on the opposite side of our transformer at 17W to 18W because they are overloaded. Secondary and main snubbers minimize external voltage limitations and losses. When in use, switching equipment increases current, resulting in a voltage surge when turned off. When considering this circumstance, optimize circuit efficiency by using the appropriate snubber settings.

2.THEROTICAL METHOD

Figure 1 depicts a standard flyback converter. The converter's components include a Mosfet Q1, a Schottky diode D1, an n-turn transformer TR, an LM magnetizing inductance, and an output capacitor C. Mosfets are

also valuable since they can function at high frequencies with little power. The recommended flyback converter uses discontinuous conduction mode.

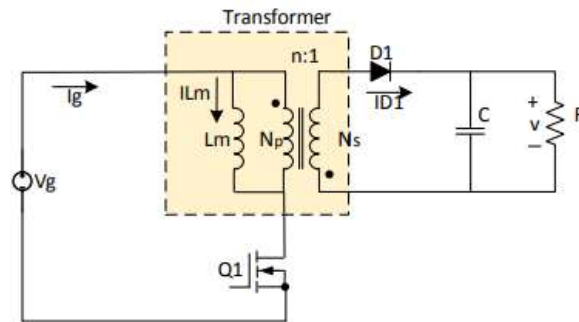


Figure 1.The conventional flyback converter

Operation Stages

Within the proposed flyback, one switching phase (T_s) consists of three discrete intervals. Power is initially delivered to the load using only the reset magnetizing inductance and output capacitor.

Stage 1 ($t_0 < t < t_1$)

The switch is activated by a Mosfet control signal sent to the gate terminal. The current flowing through the magnetizing inductance correlates directly with the rise in input voltage V_g .

$$i_{Q1} = i_{LM} = \frac{V_g}{L_M} t \quad (1)$$

The magnetizing current is i_{LM} , while the magnetic inductance is L_M . Furthermore, the magnetizing current corresponds to the switch current. When the switch is turned off, the interval terminates.

Stage 2 ($t_1 < t < t_2$)

At the start, i_{Q1} is 0, and i_{D1} is I_{D1_max} . Switch off and activate $D1$ to start this phase. Magnetization energy is passed to the output. During this time,

$$i_{D1} = I_{D1_max} - \frac{V}{L_s} t \quad (2)$$

$$I_{D1_max} = I_{LM_max} n \quad (3)$$

are definitely legitimate. The following formulas depict the transformer's secondary windings (L_s), the maximum current flowing through the diode (I_{D1_max}), and the transformer's main and secondary windings turns ratio (n). This time ends when the diode's current hits zero. As a result, the negative consequences of reverse recovery are mitigated.

Stage 3 ($t_2 < t < t_3$)

The interval begins when the diode current hits zero. The magnetizing inductance's energy is reset at this point. This phase terminates when the control signal is applied to the $Q1$ switch.

Design Procedure

Before you begin building a DC-DC converter circuit, you must first select the parameters that will provide

the desired output values. The switching element's maximum, minimum, and operating frequencies, the line frequency from which the supply voltage is derived, the desired power output, the specified exit and efficiency values for comparing input powers, the circuit's control and operation modes (discontinuous or continuous), and the loss and ripple factors must all be determined and calculated. The next section examines design features. This page discusses snubber circuit development.

Input Analysis

The impulse waveform of the input voltage is shown in Figure 2. The charging period of the input capacitor is represented by the symbol t_C . V_{AC} denotes the line voltage's RMS value.

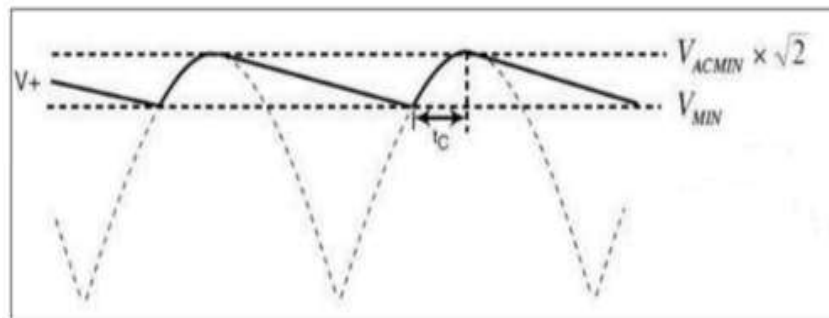


Figure 2.The input capacitor voltage waveform

Calculate this converter's input rectifier capacitor using the formula below. A calculation starts with input power and continues.

$$P_i = \frac{P_o}{\eta} \quad (4)$$

We assume that the line frequency is f_L , the input capacitor is defined as in the given equation.

$$C_{in} = \frac{P_i \left(\frac{1}{f_L} \right) - 2t_C}{(V_{AC\max}^2 - V_{AC\min}^2)} \quad (5)$$

Transformer Analysis

Consider the constrained action between DCM and CCM to calculate inductance. This inductance number refers to the transformer's magnetizing or primary winding. Calculate using the formula based on the maximum load.

$$L_{M_max} = \frac{(V_{AC_min} D_{max})^2}{2P_i f_s}$$

In this equation, f_s represents the switching frequency, while maximum load, minimum input voltage, and bound current mode can be used to calculate D_{max} , which is the maximum duty cycle in the worst-case scenario. Once f_s and P_i have been determined, calculating L_M is straightforward. DCM operation is guaranteed in applications where inductance values are less than the calculated value. The turn ratio is calculated using the Voltage-Second balance equations, as well as the primary and secondary winding

voltages. When the reflected to primary winding voltage VR value is set too high, the conversion rate increases significantly. As a result, the voltage stress on the output diode decreases, while the voltage stress on the mosfet increases. Choosing an excessively low value will result in a low conversion rate, which has the opposite effect. In this way, the turns ratio n can be calculated.

$$n = \frac{V_R}{V_o} \quad (7)$$

If it is determined that the diode is not ideal, VR must be replaced with VR+Vdiode. Air gap size has a greater influence on leakage inductance. As a result, formulas exist for calculating the airgap, assuming that the core Al is 4700nH/n².

$$\Phi = B \times A_c \quad (8)$$

where Ae, or the cross-sectional area of the E20 cores utilized in our proposed converter, is 18 mm². The formula for determining the number of turns in the primary winding is as follows:.

$$N_{p_min} = \frac{L_m I_{LM_max}}{B A_c} \quad (9)$$

Also the leakage inductance is defined as follows, where ℓ_g is the length of the air gap.

$$L_{lk} = \mu_o A_c \frac{N_p^2}{L_p \ell_g} \quad (10)$$

Snubber Analysis

The snubber components are calculated taking into account the semiconductor's resonances and ripples. The primary snubber is chosen based on the energy of the leakage inductance. The primary snubber parameter is easily configurable, and selecting an appropriate leakage inductance can reduce the snubber's power loss.

The engineer chose this primary snubber voltage based on his previous experiences with VR voltages greater than 50 V. The resistor can be calculated as shown below.

$$P_{loss_Rs} = \frac{(V_R + 50)^2}{R_s} \quad (11)$$

A light snubber, the other snubber, is connected in parallel with semiconductors. It is computed using the resonance that remains after the semiconductors are deactivated. They are used in industrial systems because of their past performance, but they cause external losses and voltage spikes. As a result, the calculated snubber values are both cost-effective and highly efficient. The resonance frequency (ω_r) can be used to calculate the following. The parameters for the snubber are Cs1 and RS1.

$$\omega_r = \frac{1}{\sqrt{L_{lk} C_{s1}}} \quad (12)$$

$$R_{s1} = X_{L_{lk}} = \omega_r L_{lk} \quad (13)$$

$$X_{Cs1} = \frac{R_{s1}}{5} = \frac{1}{\omega_r C_{s1}} \quad (14)$$

Once the leakage inductance is calculated the snubber parameters can be calculated easily.

Output Analysis

The expressions below represent the maximum duty cycle value (DMAX), the voltage ripple at the output V0, and the switching frequency (fs). Furthermore, the current ripple in the circuit has a significant impact on the capacitance at its output. Additionally, this capacitor has a low ESR. Capacitors with ESRs eliminate the need for additional filters.

$$C_o = \frac{D_{MAX} P_o}{f_s \Delta V_o V_o} \quad (15)$$

3.EXPERIMENTAL RESULTS

Table I shows how to use the design procedure described above to determine the converter's parameters. This converter's application is TOPS249witch.

Table 1. Parameters of the implementation circuit

Parameter	Symbol	Values	Model
Input Voltage	V _{AC}	85 V-265 V	-
Output Voltage	V _o	12 V(1A) and 5V (1A)	-
Output Power	P _o	17 W	-
Switching Frequency	f _s	66 kHz and 133 kHz	-
Filter Capacitor	C _i	47 μF	Elektrolytic
Output Capacitor	C _o	470 μF	Elektrolytic
Primer Inductance	L _p	3500 μH	
Leakage Inductance	L _{lk}	3,5 uH	E20 core Np=127 Ns1=13 Ns2=6
Seconder Inductance	L _s	400 μH 100 μH	

The simulation circuit scheme is given in Figure 3.

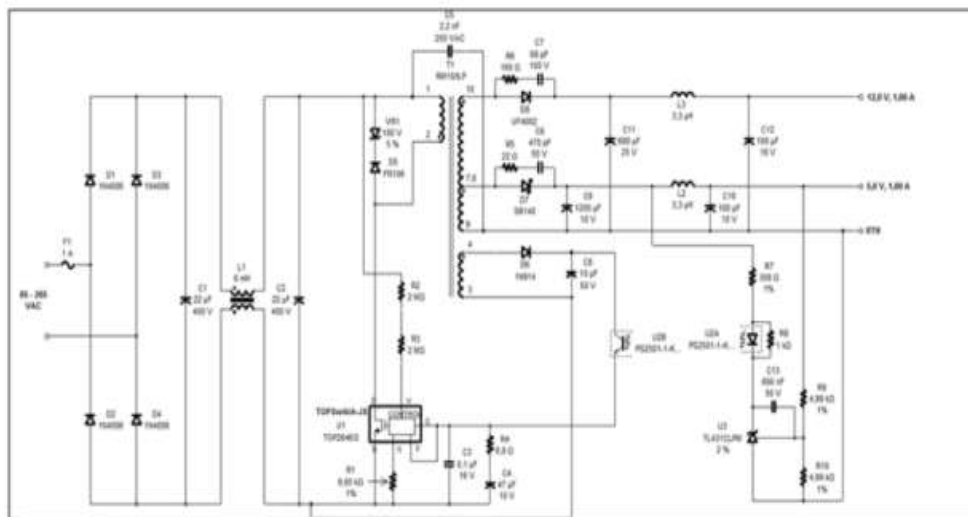


Figure 3. The simulation circuit scheme of the proposed flyback

Figure 4 depicts a prototype for the proposed converter. The snubber cell effectively reduces circuit size while preserving volume regulation.

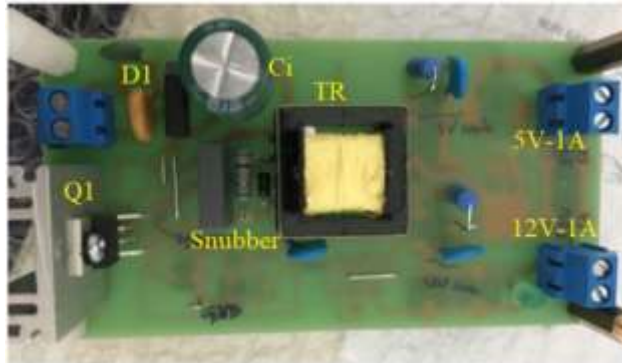


Figure 4. The prototype of the proposed flyback

The initial voltage waveforms are shown in Figure 5. To reduce switch voltage stress, use the optimal snubber cell (2W 10Ω) with 2.2 nF diodes and 100 nF primary winding, as per the design procedure.



a)



b)

Figure 5. The voltage waveform of the switch a) without snubber, b) with snubber(150V/div)

The voltage waveforms of the diode are recorded and shown in Figure 6. Undoubtedly, selecting the best snubber cell reduces voltage strains on the diode from 80.4 V to 72.8 V.



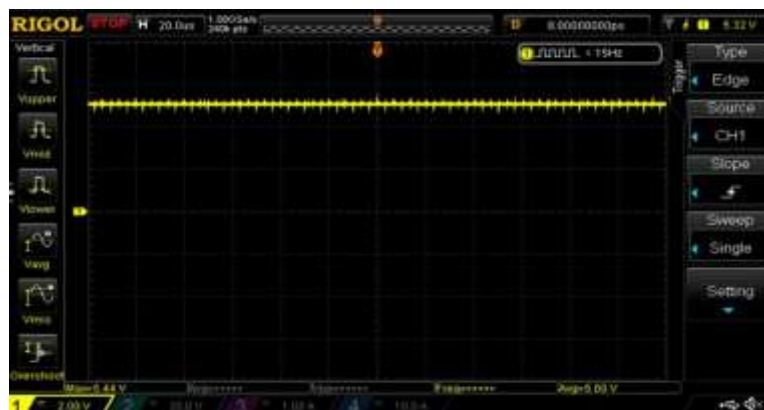
a)



b)

Figure 6. The voltage waveform of the diode a) without snubber, b) with snubber(150V/div)

Figure 7 shows the waveforms of the output voltage. The output voltages are accurately regulated using the feedback control scheme and the TOPswitch 247.



a)



b)

Figure 7. The voltage waveform of the outputs a) 5V b) 12 V

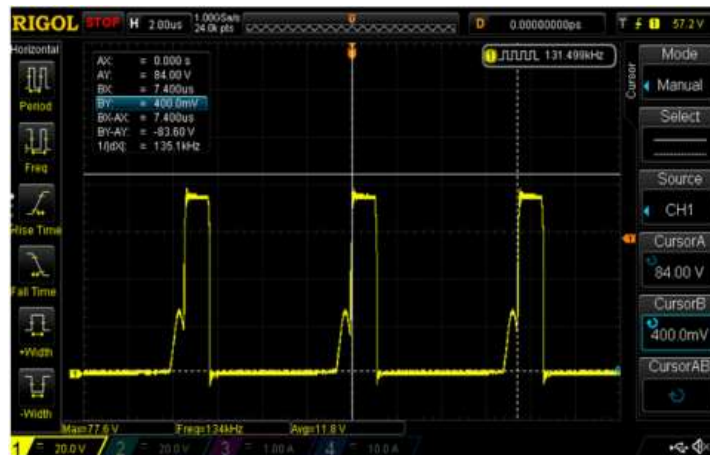
Figure 8 depicts the voltage waveforms for the switch and diode voltages at 138 kHz. The absence of external voltage stresses suggests that the proposed snubber cell is suitable for a wide range of frequencies where external losses are possible

4. CONCLUSION

The purpose of this study is to investigate and design a flyback converter with appropriate snubber cells. This study validates the comprehensive theoretical analysis by successfully implementing an application circuit with two outputs, one delivering 5V-1A and the other 12V-1A. The circuit uses an input voltage of 310V DC and frequencies of 66 kHz and 138 kHz. Increasing the switching frequency while using passive snubbers may cause additional external pressures and inefficiencies. As a result, it may be necessary to use soft switching cells externally. The snubber circuit in this study operates autonomously across various frequencies, without the use of any external soft switching cells. The prototype was used to validate the theoretical analysis and design process, with input voltages ranging from 85 V to 265 V RMS. As a result, the snubber circuits on the secondary side of our transformer are under excessive load, allowing for disassembly when the operational power reaches 17-18 Watts. The primary and secondary snubber parameters are carefully selected to reduce stress and losses caused by external voltage. The snubber's efficiency is certified at 77% due to its low power losses. Furthermore, the diode and switch experience reduced voltage stresses.



a)



b)

Figure 8. The voltage waveform of a) the switch and b) the diode

REFERENCES

1. Wang Y., J. Alonso M., Ruan X., (2017), A review of LED drivers and related technologies, *IEEE Trans Industrial Electron.*, 64 (7), 5754-5765.
2. Badawy M. O., Sozer Y., and Abreu-Garcia J. A. De, (2016), A novel control for a cascaded buck-boost PFC converter operating in discontinuous capacitor voltage mode, *IEEE Trans. Ind. Electron.*, 63(7), 4198–4200.
3. Akin B., (2020), Snubber circuit application for power factor correction flyback led driver, *Electrica*, 20(1), 108-116.
4. Chiu H.-J., Lo Y.-K., Chen J.-T, Cheng S.-J., Lin C.-Y., and Mou S.-C., (2010), A high- efficiency dimmable LED driver for low-power lighting applications, *IEEE Trans. Ind. Electron.*, 57(2), 735–743.
5. Park C. B., Choi B. H., Cheon J. P., Rim C. T., (2014), Robust active LED driver with high power factor and low total harmonic distortion compatible with a rapid-start ballast, *J Power Electron*, 14(2), 226-36.
6. Bakan A. F., Aksoy I., and Altintas N., (2012), Loss analysis of half bridge dc-dc converters in high-current and low-voltage applications, *World Academy of Science, Engineering and Technology*, 63,

201–205.

7. Poorali B., Adib E., Farzanehfard H., (2017), A Single-Stage Single-Switch Soft- Switching Power-Factor-Correction LED Driver, *IEEE Trans. Power Electron.*, 32(10), 7932-40.
8. Weidong N., Zongguang Y., Haibing W., Bin G., Long T., Lihang Y., A PSR single-stage flyback LED driver with simple line regulation and quasi-resonant operation, *J of Semiconductors*, vol.35, no.8, pp. 1-6, Jan., 2014.
9. Naresh K., Umavathi M., and Mohan H., 2014, Multi output flyback converter with switching/linear post regulators, *International Journal of Recent Development in Engineering and Technology*, 2(6), 21–26.
10. Cheng C. A., Cheng H.L., Yang F.L., Ku C.W., (2011), Single-stage driver for supplying high-power light-emitting-diodes with universal utility-line input voltages, *IET Power Electron.*, 5(9), 1614-1623.